

Reversible electrowetting and trapping of charge: model and experiments

H.J.J. Verheijen* and M.W.J. Prins[†]

Philips Research Laboratories Eindhoven, Prof. Holstlaan 4,

5656 AA Eindhoven, The Netherlands

November 6, 2018

Abstract

We derive a model for voltage-induced wetting, so-called electrowetting, from the principle of virtual displacement. Our model includes the possibility that charge is trapped in or on the wetted surface. Experimentally, we show reversible electrowetting for an aqueous droplet on an insulating layer of 10 μm thickness. The insulator is coated with a highly fluorinated layer impregnated with oil, providing a contact-angle hysteresis lower than 2° . Analyzing the data with our model, we find that until a threshold voltage of 240 V, the induced charge remains in the liquid and is not trapped. For potentials beyond the threshold, the wetting force and the contact angle saturate, in line with the occurrence of trapping of charge in or on the insulating layer. The data are independent of the polarity of the applied electric field, and of the ion type and molarity. We suggest possible microscopic origins for charge trapping.

*Also at: Eindhoven University of Technology

[†]email: prins@natlab.research.philips.com

Introduction

It is possible to reduce the contact angle of a droplet on a surface by applying an electric field between the conducting liquid and a counter electrode underneath the liquid [1–6] as shown in Fig. 1. This so-called electrowetting effect was observed first by Minnema [1] in 1980 using an insulator between liquid and counter electrode and by Beni [2] in 1981 with the liquid directly on the counter electrode. The electric field results in a distribution of charge that changes the free energy of the droplet, causing the droplet to spread and wet the surface. In systems with the liquid in direct contact with the solid electrode, the potential drops across a diffuse ionic double layer at the interface. In systems with an insulating layer of several micrometers thickness between the solid electrode and the liquid [1,3,4], the main voltage drop appears across the insulating layer.

In this paper, we use an insulating layer between the counter electrode and the aqueous solution to enhance the electrowetting force [3], achieving reversible wetting by a suitable top coating. Previously, limits have been observed for the voltage-induced reduction of contact angle: at high electric fields, the contact angle saturates [3, 4]. We consider the possibility that trapping of charge in or on the insulating layer affects the contact angle. We define charge to be trapped when the charge is bonded more strongly to the insulating layer than to the liquid. First, we derive the theory of electrowetting from the principle of virtual displacement. This provides a flexible method to extend Young’s equation to include the influence of an arbitrary charge distribution. We consider the case that a sheet of trapped charge is present in or on the insulating layer. Next, we present a measurement of the contact angle as a function of applied voltage and we extract the potential resulting from the trapped charge as a function of applied voltage. Finally, we suggest possible microscopic origins for trapping of charge.

Electrowetting model

Virtual displacement, no trapped charge.

A droplet spreads until it has reached a minimum in free energy, determined by cohesion forces in the liquid and adhesion between the liquid and the surface. In general, the energy required to create an interface is given by γ , the surface tension [N/m] or surface free energy [J/m²]. In case of an applied potential, a change in the electric charge distribution at the liquid/solid interface changes the free energy. We define our thermodynamic system as the droplet, the insulating layer, the metal electrode and the voltage source. Throughout the entire derivation, we assume that the system is in equilibrium at constant potential V . We focus on the change in free energy due to an infinitesimal increase in base area of the droplet on the solid surface, surrounded by vapor. When a potential V is applied, a charge density σ_L builds up in the liquid phase and induces an image charge density σ_M on the metal electrode. Figure 2(a) shows the edge of a droplet and its virtual displacement. An infinitesimal increase of the base area dA results in a contribution to the free energy from the surface energies as well as an energy contribution due to the additional charge density $d\sigma_L$ in the liquid and its image charge density $d\sigma_M$ on the metal electrode. The voltage source performs the work, dW_B . The free energy (F) of the system can be written in differential form:

$$dF = \gamma_{SL}dA - \gamma_{SV}dA + \gamma_{LV}dA \cos \theta + dU - dW_B , \quad (1)$$

where U is the energy required to create the electric field between the liquid and the counter electrode. The parameters γ_{SL} , γ_{SV} and γ_{LV} are the free energies of the solid/liquid, solid/vapor and liquid/vapor interface respectively for the situation in the *absence* of an electric field. The contact angle, θ , is the angle between the liquid/vapor interface and the solid/liquid interface at the contact line (see Fig. 1) [7]. Mechanisms for energy dissipation, which may cause contact-angle hysteresis, are not taken into account.

Let us first consider the situation in the absence of an externally applied voltage, so $dU = dW_B = 0$. When $dF/dA = 0$, we find the minimum in free energy, relating the surface energies to the contact angle. This equation was obtained by Young [8] in 1805:

$$\gamma_{LV} \cos \theta = \gamma_{SV} - \gamma_{SL} . \quad (2)$$

For a non-zero potential, we have to include the energy of the charge distribution. In Fig. 2(a), the droplet with charge density σ_L is at constant voltage V , while the metal electrode with charge density $\sigma_M = -\sigma_L$ is at ground potential. The electrostatic energy per unit area below the liquid is given by:

$$\frac{U}{A} = \int_0^d \frac{1}{2} \vec{E} \vec{D} dz , \quad (3)$$

where z is the coordinate perpendicular to the surface, d the thickness of the insulating layer, \vec{E} the electric field and \vec{D} the charge displacement, with $\vec{D} = \epsilon_0 \epsilon_r \vec{E}$ [9]. The increase of free energy due to the charge distribution in the liquid, upon an infinitesimal increase of droplet base can be written as:

$$\frac{dU}{dA} = \frac{1}{2} d E D = \frac{1}{2} d \frac{V}{d} \sigma_L = \frac{1}{2} V \sigma_L . \quad (4)$$

The electric field originating from the liquid/vapor boundary of the droplet (the so-called fringing or stray field) makes a constant contribution to the free energy: this contribution remains unaltered when the contact line is displaced by dA . Therefore, the stray fields do not contribute to dU . The voltage source performs the work to redistribute the charge; per unit area the work is given by [10]:

$$\frac{dW_B}{dA} = V \sigma_L . \quad (5)$$

Calculating the minimum of free energy, we get Young's equation with an additional electrowetting term γ_{EW} , the electrowetting force per unit length due to the applied potential:

$$\gamma_{LV} \cos \theta = \gamma_{SV} - \gamma_{SL} + \gamma_{EW} , \quad (6)$$

with the electrowetting force:

$$\gamma_{EW} = \frac{1}{2} \frac{d}{\varepsilon_0 \varepsilon_r} \sigma_L^2, \quad (7)$$

where we used $\sigma_L = \varepsilon_0 \varepsilon_r V/d$ (Gauss' law), with ε_r the dielectric constant of the insulating layer and ε_0 the permittivity of vacuum. We can rewrite Eqs.(6) and (7) to get the well-known relation between θ and V for electrowetting [3–5]:

$$\gamma_{LV} [\cos \theta(V) - \cos \theta_0] = \frac{1}{2} \frac{\varepsilon_0 \varepsilon_r}{d} V^2, \quad (8)$$

where θ_0 is the contact angle at zero volt.

Influence of charge trapping.

When we apply a potential difference between the liquid and the metal electrode, electric forces work on the ions in the liquid and pull them toward the insulating layer. There is a possibility that charge becomes trapped in or on the insulating layer when the interaction of the ions with the solid is stronger than with the liquid. In the three-phase region, ions are trapped when the de-trapping time is large compared to the typical vibration times of the contact line. As a result of excitations of the droplet, e.g. thermal, mechanical or voltage-induced vibrations, a density of trapped charge arises on both sides of the contact line.

As yet we do not specify the precise nature of the trapped charge (e.g. electronic or ionic); we simply assume that a layer of charge with constant surface charge density σ_T is trapped in the insulating layer at distance d_2 from the top of the insulator as shown in Fig. 2(b). To determine the change in electrostatic energy due to the infinitesimal base area increase [dU in Eq.(1)], we have to take into account the electrostatic contribution below the liquid dU_L , as well as the contribution below the vapor phase, dU_V :

$$dU = dU_L - dU_V. \quad (9)$$

The sign difference is due to the fact that the virtual displacement dA increases the solid/liquid interface while the solid/vapor interface is decreased. We assume that the trapped charge is distributed uniformly at constant depth, extending sideways to the left of the contact line to a length scale of at least the insulator thickness. Then, the charge density at the liquid/vapor interface due to fringing fields at the edge of the droplet is unaltered by the virtual displacement. Therefore, we omit the electrostatic energy of the fringing field in Eq.(9).

The potential as a function of the depth in the insulator is sketched in Fig. 3(a). The solid line shows the potential in the absence of trapped charge. For the case of charge trapping, the potential beneath the liquid phase is indicated by the long dashed line while the short dashed line shows the potential beneath the vapor phase. The vertical line indicates the depth where the trapped charge is situated. Figure 3(b) shows a plot of the electrostatic fields, with $E = -\nabla V$. It is clear that trapping of charge lowers the electric field at the liquid/solid interface and should consequently reduce the electrowetting force. The charge density of the trapped charge, σ_T , is at potential V_T^L below the liquid and at V_T below the vapor phase. On the metal electrode below the liquid, the charge density is $\sigma_M^L = -(\sigma_L + \sigma_T)$. The charge density on the metal electrode below the vapor phase is $\sigma_M^V = -\sigma_T$. Using the general expression for the energy density [Eq.(3)], we find the electrostatic energy density below the liquid phase:

$$\begin{aligned}
\frac{dU_L}{dA} &= \frac{1}{2}d_1E_1D_1 + \frac{1}{2}d_2E_2D_2 \\
&= \frac{1}{2}d_1\frac{V_T^L}{d_1}(\sigma_T + \sigma_L) + \frac{1}{2}d_2\frac{V - V_T^L}{d_2}\sigma_L \\
&= \frac{1}{2}V_T^L\sigma_T + \frac{1}{2}V\sigma_L .
\end{aligned} \tag{10}$$

The energy to create the charge distribution below the vapor phase equals:

$$\frac{dU_V}{dA} = \frac{1}{2}d_1\frac{V_T}{d_1}\sigma_T = \frac{1}{2}V_T\sigma_T . \tag{11}$$

The work performed by the voltage source per unit area is given by Eq.(5). Using Gauss' law, we find the following relationships between the charge densities and the potentials:

$$\sigma_T = \frac{\varepsilon_0 \varepsilon_r V_T}{d_1} \quad (12)$$

$$\sigma_L = \frac{\varepsilon_0 \varepsilon_r (V - V_T)}{d} \quad (13)$$

$$V_T^L = V_T + \frac{d_1}{d} (V - V_T) . \quad (14)$$

Using Eq.(1), Eq.(5), Eqs.(9)–(14) and $dF/dA = 0$, we recover Eqs.(6) and (7), the modified Young equation. With Eq.(13), we find the following relation for the contact angle modulation in the presence of trapped charge:

$$\gamma_{LV} [\cos \theta(V) - \cos \theta_0] = \frac{1}{2} \frac{\varepsilon_0 \varepsilon_r}{d} (V - V_T)^2 . \quad (15)$$

The electrowetting force is proportional to the square of the applied voltage minus the voltage due to charge trapping. This causes a reduction of the electrowetting force.

Results

We used a system as shown in Fig. 1. On a silicon substrate, a conducting aluminum layer (100 nm) and an insulating layer of parylene-N (10 μm , $\varepsilon_r = 2.65$, chemical vapor deposited as in Ref. [4]) were applied. Subsequently a thin hydrophobic AF1600 top coating [11] was deposited by spincoating a 0.1 wt% solution of AF1600 (DuPont) in FC726 (3M) at 1000 r.p.m. during 30 s, resulting in a layer of approximately 30 nm thickness. In order to obtain a low contact-angle hysteresis, we impregnated the coating with silicon oil. The sample was left in silicon oil for several hours. Before the experiment the excess of oil was removed; this is possible because the contact angle of silicon oil on AF1600 is about 40° [12]. The in-liquid electrode was a platinum wire. The droplet consisted of 10 μl of an aqueous solution, with 1.0 M, 0.1 M, 0.01 M KCl or 0.1 M K₂SO₄.

The capacitance was measured between the platinum electrode and the metal counter electrode as a function of applied voltage, using a 700 Hz, 5 V ac-signal which was superimposed on the dc-voltage. The capacitance gives a measure of the contact area between liquid and surface and is shown in Fig. 4(a). The potential of the liquid was increased to 500 V and subsequently decreased to 0 V; the opposite voltage polarity was measured on a different spot to avoid possible interference with previously trapped charge. The time interval between measurement points (1 s) was more than an order of magnitude longer than the time required for spreading of the droplet (experimentally verified to be about 20 ms [13]). We find that the droplet base increases by nearly a factor of three due to the applied voltage. The droplet recovers its original shape upon removal of the electric potential. Measurements with the solutions of different molarities and ion types resulted in identical curves.

The contact angle θ was derived from the measured capacitance, using the known dielectric constant and thickness of the insulating layer, the droplet volume and the droplet shape. This electrical measurement method gives the contact angle with an accuracy of 2° ; details are described in Ref. [13]. Figure 4(b) shows the contact angle, derived from the capacitance measurement along with the theoretical curve according to Eq.(8). The contact-angle hysteresis is less than 2° . To our knowledge, such a high degree of reversibility has not yet been reported in electrowetting experiments. We attribute the low value of contact-angle hysteresis to the penetration of the oil into nano-pores of the amorphous fluoropolymer layer [11], which reduces the already very low surface heterogeneity of the top coating (for water on non-impregnated AF1600, the contact-angle hysteresis is about 7°). At zero volt, the value of the contact angle on the impregnated surface agrees well with the advancing contact angle on the non-impregnated surface. This indicates that the fluoropolymer determines the surface energy rather than the silicon oil.

We can distinguish two regions in the plot. In the region $-240 < V < 240$ V, the measured contact angle is consistent with the theoretical contact angle of Eq.(8) within 2° . According to our model [Eq.(15)], this means that at low voltages the ionic charge remains in the liquid without being trapped on or in the insulating layer. Within this voltage range we demonstrated reproducible droplet spreading for more than 10^5 times. At higher voltages, we notice contact-angle saturation at about 60° and differences between the advancing and receding curves. To investigate the possibility that the saturation of contact angle is caused by trapping of charge, we applied a voltage higher than 240 V to the droplet and while maintaining the applied voltage, adsorbed the liquid into a tissue. Afterward, when blowing humid air across the sample, we observed a condensation pattern [3] at the position and in the shape of the droplet base. During subsequent electrowetting experiments in this area, we detected a nonzero electrostatic potential, having the sign of the previously applied potential, which points at the presence of charge. Therefore, we attribute the condensation pattern to the preferential deposition of polar water molecules on the charged area of the surface. Finally, we noticed a decrease of the electrostatic surface potential after a large grounded droplet was placed on the charged coating; no decrease of the potential was observed when the large droplet was electrically floating. These experiments prove that contact-angle saturation is accompanied by charging of the insulating coating. The charge can be removed by an electrical shortcut between the metal electrode and the surface of the insulator.

We have analyzed the data of Fig. 4 with our model for voltage-induced wetting in the presence of trapped charge [Eq.(15)]. We ascribe the difference between the measured contact angle and the contact angle of the old model [Eq.(8)] to the voltage of trapped charge (V_T). Figure 5(a) shows the resulting plot for V_T . We notice a threshold voltage V_{th} of 240 ± 10 V. For $|V| < V_{th}$, the voltage of trapped charge equals zero and the electrowetting force $\gamma_{EW} \propto V^2$.

For $|V| > V_{th}$, $V_T \approx V - V_{th}$ and $\gamma_{EW} \propto (V - V_T)^2$. This means that above the threshold voltage, almost all charge added by the voltage source gets trapped in or on the insulating layer. Figure 4(b) shows the charge density in the liquid phase σ_L . For voltages below the threshold, σ_L increases linearly with increasing applied voltage. Beyond the threshold voltage, σ_L remains approximately constant, in line with the saturation of the contact angle.

Discussion and Conclusions

The data of the previous section show a threshold-like saturation behavior for the electrowetting force and for the charge density in the liquid. The voltage of trapped charge shows a linear increase beyond the threshold voltage. The curves are symmetric for positive and negative potential, and independent of the ion type, ion valence and ion molarity that we have tested. Furthermore, the advancing curve is consistent with the receding curve, indicating that the trapped charge is released upon lowering of the applied voltage.

Let us now consider possible microscopic origins for trapping of charge. We defined trapped charge as charge which has a stronger interaction with the insulating layer than with the liquid. Clearly, the underlying charge bonding mechanism cannot have a chemical nature, as an expected dependence on voltage polarity, ion type, valence and molarity was not observed. Charge trapping could occur due to the attractive electrostatic force between ions in the liquid and the metal counter electrode. When the electrostatic force on the ion exceeds the force between the liquid and the ion, it moves toward the insulating layer and remains in or at the insulating layer [14]. The ion might exchange some of its hydration shell for a bond with the surface. Although this model predicts a threshold-like trapping behavior, a dependence on the valence of the ions is expected, in disagreement with our experimental results.

At the threshold electric field, the electrowetting force is of the same order

of magnitude as or larger than the surface tensions in our system (for $V = 240$ V, $\gamma_{EW} = 68$ mN/m). Therefore, we propose that it is possible that instabilities in the liquid/solid interface or the liquid/vapor interface occur. Small charged droplets or molecular clusters could move into nano-pores of the insulating layer and become trapped. In this concept, no dependence on molarity, ion type, valence of the ions or polarity of the applied field is expected. While this line of thought seems in agreement with the behavior of V_T (a threshold and subsequently a slope close to one), further research is needed to determine the microscopic mechanisms of charge trapping.

In conclusion, the principle of virtual displacement provides a transparent method to calculate the influence of an arbitrary charge distribution on the contact angle. The virtual change of electric energy is calculated by integrating the energy density of the electrostatic field. Using this method, we derived a model for electrowetting that accounts for a reduction of the electrowetting force by the assumption that charge is trapped in or on the insulating layer [Eq.(15)].

We demonstrated reversible electrowetting using an aqueous droplet on a sample with a 10 μm thick parylene insulating layer and a highly fluorinated hydrophobic AF1600 top coating which was impregnated with silicon oil. The measured contact-angle hysteresis was below 2° . For voltages between -240 V and 240 V the charge remains in the liquid and is not trapped in or on the insulating layer. At higher voltages, charge gets trapped with a threshold-like behavior, limiting the charge density that can be induced in the liquid. We observed that charge remains at areas where the droplet has receded in a high-voltage state and that discharging of the surface is possible with a zero-voltage droplet. For all solutions tested, the absolute value of the threshold voltage is independent of the polarity of the applied voltage, the ion type, ion molarity and ion valence (Cl^- vs. SO_4^{2-}).

From an experimental standpoint, the distribution of the trapped charge

should be measured quantitatively with for instance a scanning Kelvin probe. This will clarify the dependence of the trapped charge density on the applied voltage and on the distance with respect to the contact line. The mechanisms of de-trapping of charge are interesting and need to be studied in more detail. The dependence of the threshold electric field on the insulator thickness, measured for different salts, solvents and top coatings may provide information on the mechanisms that cause the trapping of charge. Eventually, when trapping of charge in the insulator can be avoided, it may become possible to reversibly reach complete wetting of a surface by an applied electric potential.

Acknowledgement

We thank W. Welters and A. Kemmeren for coating preparation and for valuable discussions.

References

- [1] Minnema, L.; Barneveld, H.A.; Rinkel, P.D. *IEEE Trans. Electr. Insul.* **1980**, *EI-15*(6), 461.
- [2] Beni, G.; Hackwood, S. *Appl. Phys. Lett.* **1981**, *38*(4), 207.
- [3] Vallet, M.; Berge, B.; Vovelle, L. *Polymer* **1996**, *37*(12), 2465.
- [4] Berge, B. *C.R. Acad. Sci. Paris, Ser. II* **1993**, *317*, 157. Welters, W.J.J.; Fokkink, L.G.J. *Langmuir* **1998**, *14*(7), 1535. Vallet, M.; Vallade, M.; Berge, B. *European Physics Journal B.*, submitted for publication.
- [5] Sondag-Huethorst, J.A.M.; Fokkink, L.G.J. *J. Electroanal. Chem.* **1993**, *367*, 49.

- [6] Abbott, N.L.; Gorman, C.B.; Whitesides, G.M. *Langmuir* **1995**, *11*, 16. Gorman, C.B.; Biebuyck, H.A.; Whitesides, G.M. *Langmuir* **1995**, *11*, 2242.
- [7] Regardless of the macroscopic geometry of the system, it can be shown that $d\theta/dA$ equals zero. See also: Adamson, A.W.; Gast, A.P. *Physical Chemistry of Surfaces*; John Wiley & Sons, Inc.: New York, 1997, section X.
- [8] Young, T.N. *Phil. Trans. Roy. Soc. London* **1805**, *95*, 71.
- [9] Jackson, J.D. *Classical Electrodynamics*; John Wiley & Sons, Inc.: USA, 1975.
- [10] Feynman, R.P.; Leighton, R.B.; Sands, M. *The Feynman lectures on physics II*; Addison-Wesley: Reading, 1977. Section 8-2.
- [11] Resnick, P.R.; Buck, W.H. in *Modern Fluoropolymers*; Scheirs, J., Ed.; John Wiley & Sons Ltd.: Chichester, 1997.
- [12] Schneemilch, M.; Hayes, R.A.; Petrov, J.G.; Ralston, J. *Langmuir* **1998**, *14*(24), 7047.
- [13] Verheijen, H.J.J.; Prins, M.W.J. *Rev. of Sci. Instr.*, **1999**, *70*(9).
- [14] Chudleigh, P.W. *J. Appl. Phys.* **1976**, *47*(10), 4475.

Figures

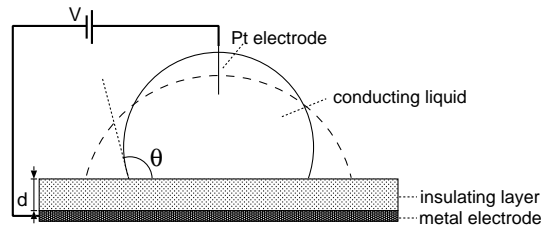


Figure 1: Schematic drawing of an electrowetting experiment. A droplet of a conducting liquid is placed on an insulating layer of thickness d , which is deposited on a metal counter electrode. Application of a potential V between the droplet and the metal electrode changes the free energy of the droplet and results in a decrease of the contact angle θ . The resulting droplet shape is indicated by the dashed line.

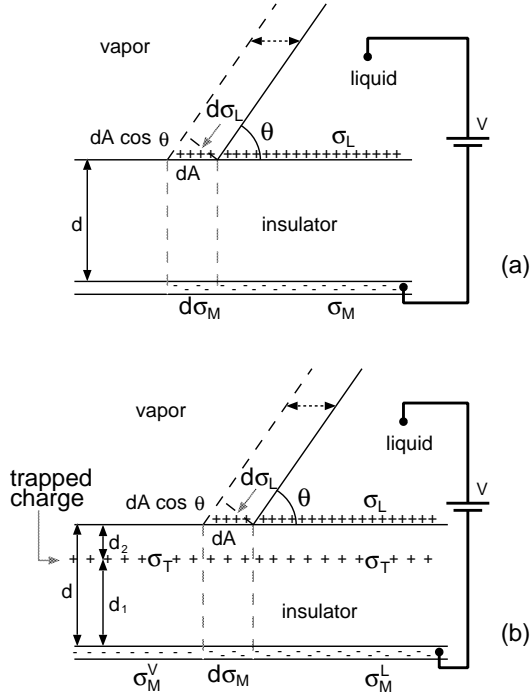


Figure 2: (a) Schematic picture of the virtual displacement of the contact line in the presence of a potential across the insulator. An infinitesimal increase in base area dA at fixed voltage V changes the free energy of the droplet, as a result of a change in interface area and the placement of additional charge $d\sigma_L$ and image charge $d\sigma_M$. (b) The virtual displacement of the contact line in the presence of a sheet of trapped charge. Now, the infinitesimal increase dA alters the free energy not only via the charge distribution between the electrode and the liquid, but also via the charge distribution below the vapor phase.

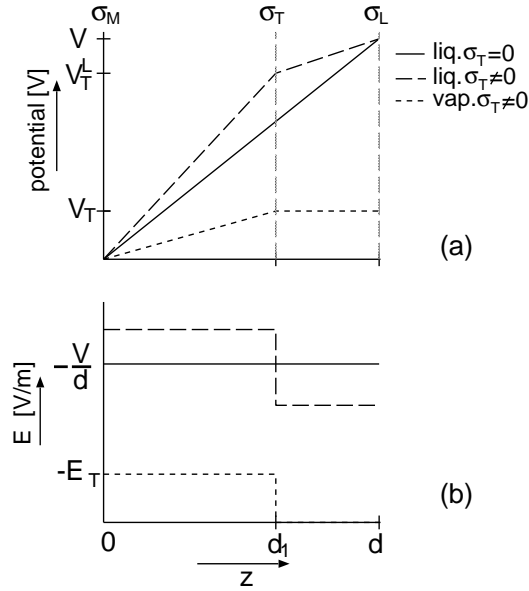


Figure 3: Sketch of the potential (a) and the electric field (b) in the insulator beneath the liquid and the vapor phase. Below the liquid phase, the potential and electrostatic field without trapped charge ($\sigma_T = 0$, solid lines) and with trapped charge ($\sigma_T \neq 0$, long dash) are shown. Below the vapor phase, the curves in the presence of trapped charge are shown (short dash). The voltage drop across the diffuse ionic double layer is neglected.

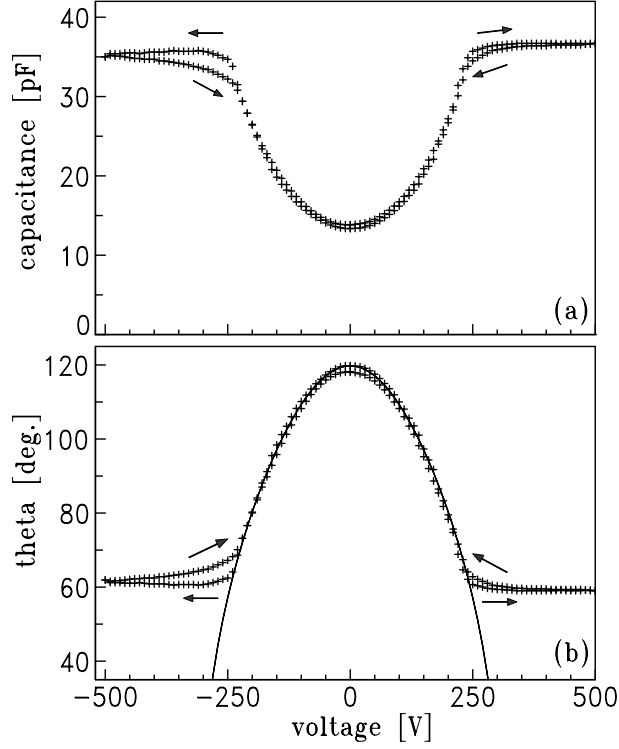


Figure 4: (a) The capacitance between a $10 \mu\text{l}$ liquid droplet and counter electrode as a function of applied dc-potential. The insulator thickness is $10 \mu\text{m}$. We used a 700 Hz ac-signal with 5 V amplitude and a sweep rate $\sim 10 \text{ V/s}$. (b) The contact angle derived from the capacitance measurement. The contact-angle hysteresis is less than 2° in the range $-240 < V < 240 \text{ V}$. For higher voltages, the contact angle saturates around 60° . The continuous line is according to Eq.(8), using $\theta_0 = 119^\circ$, $d = 10 \mu\text{m}$, $\varepsilon_r = 2.65$ and $\gamma_{LV} = 72 \text{ mN/m}$.

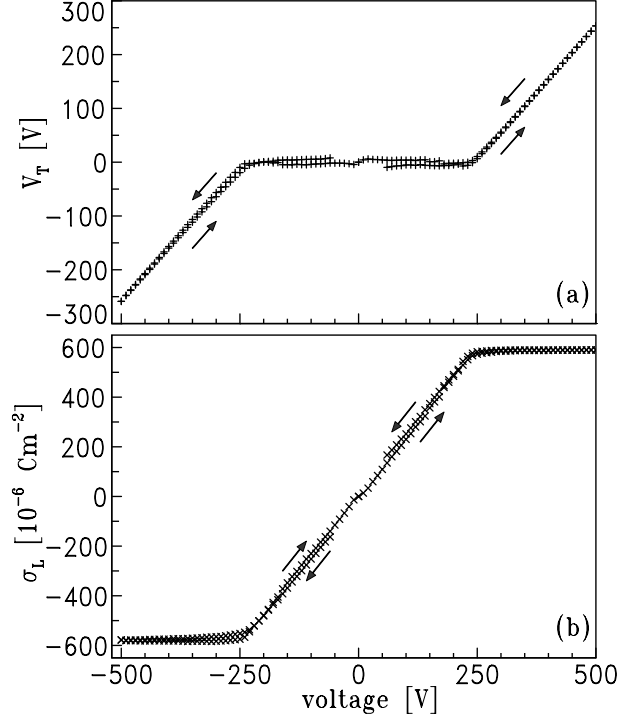


Figure 5: (a) The voltage due to trapped charge, V_T , as a function of applied potential. V_T is derived from the data of Fig. 4 and Eq.(15). For potentials below the threshold of ± 240 V, the voltage due to trapped charge equals zero; for higher potentials, charge gets trapped. (b) The surface charge density in the liquid, σ_L , calculated using Eq.(13). The charge density in the liquid increases until a threshold voltage is reached, beyond which it saturates. Note that the charge density is of the same order as 10^{-4} monolayer of unit charge.